Proceedings of the American Control Conference,
San Diego, CA, May 31-June 2, 2023

A Transmission Rate Estimator & Controller for Infectious Disease SIR Models - Constant Case

Enrique Barbieri[1] Vassilios Tzouanas[2]

***Abstract*— A widely studied susceptible $S(t)$, infectious $I(t)$, and removed $R(t)$ (SIR) family of deterministic, lumped-parameter models of directly transmitted infectious diseases is considered to estimate the transmission rate assumed to be piecewise constant via a linear, extended-state observer. Then, although the transmission rate is not a control signal in the traditional sense, the application of feedback control design offers guidance in implementing mitigating actions that curb the disease spread. A linearized model at each measurement point is used for offline observer design with the transmission rate treated as an unknown but constant disturbance. The observer-based controller simulations in discrete time explore heuristic policies that may be implemented by public health and government organizations.**

I. INTRODUCTION

Interest in controlling infectious diseases caused by bacteria, viruses, and fungi continues to rise particularly due to the COVID-19 pandemic of the last three years. This pandemic has tested in new ways the world's ability to record, store, share and display critical metadata in an effort to facilitate communication [1]. Many mathematical models can be found in the literature, but the most basic comprises three states denoting the susceptible (S), infectious (I), and removed (recovered and deceased) (R) sub-groups of the total population N known as the SIR model [2]. Its complexity is increased in various ways, for example, by segmenting the population fractions for finer resolution, considering spatiotemporal spreading, exploring time-dependent parameters, and extending to stochastic modeling [3]-[11].

A great deal of effort is devoted to using real data to fit model parameters and assist with prediction [11], [12]. Optimal control strategies for SIR models have been explored in various settings [13]-[19]. The simplicity of linear models [20], [21] however is ideal in gaining insights into the infection spread behavior and in guiding toward the design of health, economic and societal actions that deter the disease spread. We continue along the lines in [21] with two observations summarized below. To our knowledge, the framework described in this paper has not been reported in the literature.

A. Family of Models

A family of SIR-type models can be written as

$$\dot{z}(t) \quad = \quad G(t)z + F(z)v(t) \tag{1}$$

where $z = [z_1 \ z_2 \ z_3 \cdots z_n]^\top$ is the state, $v(t)$ is the transmission rate; F is a vector of nonlinear functions; and matrix G is in general time-varying but could be constant or piecewise constant.

B. Modeling for Feedback Control

Denote by $a(t) = [a_1 \ a_2 \ \cdots a_m]^\top$ a set of mitigating actions that may include pharmaceutical and non pharmaceutical interventions such as full or partial mandates on mask wearing, social distancing by age group, business and school closures, contact-tracing protocols, travel restrictions, application of vaccination and therapeutics, and various economic, legal, or political measures. The actions are followed by tracking of new infections to estimate the change in transmission rate $v(t)$ and adjust the management of $a(t)$ accordingly.

Despite the fact that $v(t)$ is not a control input in the traditional sense, Figure 1 illustrates how a disease-spread model (SIR) and real-time state measurements may be used to design a gold-standard $v^o(t)$ mapped to a set $a(t)$ which is scheduled by policy makers using all available information.

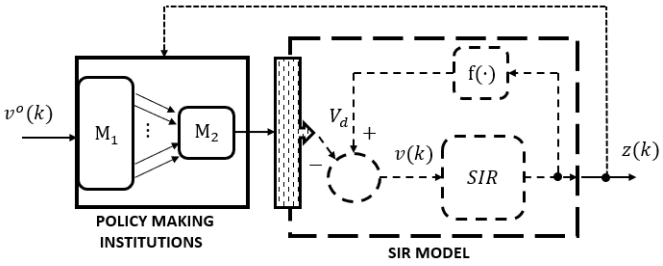

Fig. 1. Idealized SIR model under Control $v^o(k)$

Hence, assume further that there are relations

$$a(t) \quad = \quad M_1[z(t-t_{d1}), v^o(t-t_{d2})] \tag{2}$$
$$v(t) \quad = \quad M_2[a(t-t_{d3}), z(t-t_{d4})] \tag{3}$$

where M_1, M_2 are maps to be determined, giving flexibility for the action set $a(t)$ to be designed. It is common in the literature to consider a quarantine time window of length T_q during which action set $a(t)$ is enforced based on the epidemic state at the start of T_q. In addition, maps M_1, M_2 use time delays $t_{d1} - t_{d4}$ to take into account implementation delays by policy makers, delays in the public's response due to hesitancy and other uncertainty effects.

[1] IEEE S.M., Professor, Technology Division, Cullen College of Engineering, University of Houston, Houston, TX, 77204, USA ebarbieri@uh.edu

[2] Professor & Chair, Computer Science and Engineering Technology Department, University of Houston - Downtown, Houston, TX, 77002, USA tzouanasv@uhd.edu

In this paper we focus on the normalized SIR model

$$\begin{aligned}\dot{S}(t)/N &= \dot{z}_1(t) = -z_1 z_2 v \\ \dot{I}(t)/N &= \dot{z}_2(t) = -\gamma z_2 + z_1 z_2 v \\ \dot{R}(t)/N &= \dot{z}_3(t) = \gamma z_2\end{aligned}$$

where N is the total population, $\gamma > 0$ is the recovery rate indicating that an infected individual takes on average $1/\gamma$ (time units) to recover. The states $\{z_1, z_2, z_3\}$ are the corresponding population fractions. The SIR model is discretized and linearized around an operating point under an assumed constant but unknown transmission rate $v = V_d$ during a specified time window. This leads to a state-space model where V_d enters the equations as a constant input disturbance. Hence, an extended-state Luenberger-type observer can be designed to converge to V_d. Simple relations M_1 and M_2 are selected together with the observer to develop a set of mitigating actions that steer the SIR behavior towards a desirable operating state.

The remainder of the paper is organized into three additional sections. Section II describes the control problem, assumptions, and a proposed solution. Section III illustrates the results via simulations. Section IV concludes and points to further work.

II. Control Problem

A discrete-time version of the SIR model with sampling period $T > 0$ is written as follows

$$z_1(k+1) = z_1(k) - T z_1(k) z_2(k) v(k) \quad (4)$$

$$z_2(k+1) = (1 - T\gamma) z_2(k) + T z_1(k) z_2(k) v(k) \quad (5)$$

$$z_3(k+1) = z_3(k) + T\gamma z_2(k) \quad (6)$$

Idealizing the interaction between Policy Making Institutions at the city, county or country level, and the SIR Model in an environment is depicted in Figure 1. The idealization illustrates how challenging or even impossible it is to model all nuances of how the disease spread is impacted by the policy making institutions. The actions' effectiveness suffer from implementation delays, geographical and community travel factors, as well as society's reaction such as hesitancy or outright rejection of the various measures. The depiction hints at this modeling uncertainty barrier and simply assumes a macro- or net-effect that tends to reduce the transmission rate. Lastly, the feedback of state measurements directly to the Policy Making Institutions box is shown dotted because they are not used in this paper.

The SIR dynamics are such that, in open-loop with no control, $v^o(k) = 0$, and under a constant transmission rate $v(k) = V_d$, the infectious fraction $z_2(k)$ increases to a peak and decreases to zero for all initial conditions [2], while the susceptible fraction $z_1(k)$ decreases to a final value $S(\infty)$ and the removed fraction $z_3(k)$ reaches $R(\infty)$ satisfying $z_1(k) + z_2(k) + z_3(k) = 1, \ \forall k$. In this idealization, V_d is treated as an unknown disturbance produced by some internal mechanism shown as $f(\cdot)$. In simulations, it is common to assume that when an infection starts, $S(0) = S_0 \approx 1$, $I(0) = I_0 = 1 - S_0 \approx 0$ and $R(0) = 0$. A sample response under these conditions using the model (4)-(6) is shown in Figure 2. Various analytical results along these lines were developed in [20].

Under feedback control on the other hand, the purpose of the term $M_2 M_1[v^o(k)]$ is to simulate policy actions that when implemented have the effect of reducing the effective transmission rate $v(k)$ depending on the policy action effectiveness. Some heuristic ideas were simulated for an ARMA model of a feedback-linearized SIR system in [21].

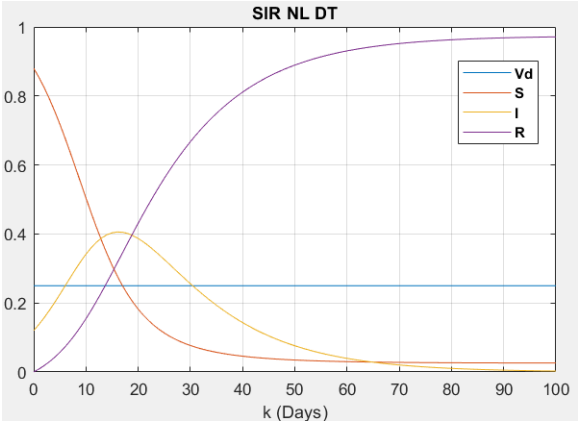

Fig. 2. SIR Nonlinear Discrete-Time in Open-Loop ($T = 1; \ \gamma = 1/14$).

In the remainder of this paper we focus on the controllable state $[z_1 \ z_2]^\top$ recognizing that $z_3(k) = 1 - z_1(k) - z_2(k)$. Finally, the SIR model predicts the disease spreads when the basic reproduction number $R_e = V_d/\gamma > 1.0$, that is when the transmission rate is larger than the recovery rate. We take advantage of this fact in the design of a proposed controller.

Control Objective

A strategy was suggested recently [17] that seeks to adjust the set of mitigating actions $a(t)$ to reduce the peak strain on intensive-care units. Then, long-term measures bring society back to pre-epidemic states. The strategy tends to reject the ON/OFF management of individual mitigating actions in $a(t)$. In fact, a simulation of an ON/OFF lock-down policy produced multiple infection waves, and a data visualization example using the Johns Hopkins CORONA Virus Resource Center correlated ON/OFF policies with detrimental consequences on cumulative infectious cases in the state of Texas between March 19, 2020 and September 10, 2021 [21].

Instead of ON/OFF, the strategy advocates policies that steer the system's operating point near $R_e \approx 1.0$ - thus achieving mitigation because then, an infectious individual spreads the disease on average to only one or fewer people. If $R_e < 1.0$ the disease does not spread and suppression is achieved.

This is an interesting strategy that deserves more attention. Hence, we design a control policy that seeks to steer the system dynamics in a direction that maintains $R_e \approx 1.0$ or equivalently, $v \to \gamma$. To that end, consider the k^{th} time window W_k comprising a number of samples during which

V_d is set to a constant but unknown value. Feedback control should produce policies that steer $v \rightarrow \gamma$ during each window.

Operating Point Definition: Referring to Figure 1, let the pair $(z_s, v_s + V_d)$ be the operating point of the idealized SIR model where, $z_s = [z_{1s}\ z_{2s}]^\top$ is the measured state at the start of time window W_k, and v_s is the input operating point. Then, set $z(k) = z_s + x(k)$ and $v(k) = v_s + V_d + u(k)$, where $x(k)$ and $u(k)$ are small deviations away from the operating point.

A small signal model valid in the vicinity of the operating point leads to

$$\begin{aligned} x(k+1) &= \Phi x(k) + \Gamma\{u(k) + V_d\} \quad (7) \\ y(k) &= c^\top x(k) \quad (8) \end{aligned}$$

where $\Phi = \begin{bmatrix} 1 - Tz_{2s}v_s & -Tz_{1s}v_s \\ Tz_{2s}v_s & 1 - T\gamma + Tz_{1s}v_s \end{bmatrix}$, $c^\top = [1\,0]$ $\Gamma = \begin{bmatrix} -1 \\ 1 \end{bmatrix} Tz_{1s}z_{2s}$, and the transmission rate V_d enters the state equations as an unknown input disturbance term. An extended-state observer is suitable to estimate V_d [22].

To that end, the augmented state $x_a(k) = [x^\top(k)\ x_d(k)]^\top$ with $x_d(k+1) = x_d(k)$, a constant, yields the state and output equations

$$\begin{aligned} x_a(k+1) &= \Phi_a x_a(k) + \Gamma_a u(k) \quad (9) \\ y_a(k) &= c_a^\top x_a(k) \quad (10) \end{aligned}$$

where

$$\Phi_a = \begin{bmatrix} \Phi & \Gamma \\ 0 & 1 \end{bmatrix}; \quad \Gamma_a = \begin{bmatrix} \Gamma \\ 0 \end{bmatrix}; \quad c_a^\top = [c^\top\ 0]$$

Such augmented-state formulation can be extended to a disturbance V_d governed by a known model, for example,

$$\nu(k+1) = \Phi_d \nu(k) \quad \text{and} \quad V_d(k) = c_d^\top \nu(k)$$

β-Control Design

Consider the idealized SIR model in Figure 1 with map relations (2)-(3), linearized model (7)-(8), and augmented-state system (9)-(10). Let $M_2^\top = w^\top = [w_1\ w_2\ \cdots w_m]$, that is, a vector of weights reflecting the effectiveness of the m mitigating actions $a = [a_1\ a_2\ \cdots a_m]^\top$.

Then, $v(k) \rightarrow \gamma$ and $R_e \rightarrow 1$ by the least-squares set of mitigating actions

$$a = \begin{cases} w(w^\top w)^{-1}(\hat{x}_d - \gamma) & \hat{x}_d > \gamma \\ 0 & \hat{x}_d \leq \gamma \end{cases} \quad (11)$$

and control

$$v^o(k) = -(u(k) + \gamma)$$

where $u(k)$ is generated by the extended-state estimator and state-feedback law

$$\begin{aligned} \hat{x}_a(k+1) &= \left(\Phi_a - Lc_a^\top\right)\hat{x}_a(k) + [\Gamma_a\ L]\begin{bmatrix} u(k) \\ y(k) \end{bmatrix} \\ u(k) &= -\left[K^\top\ 1\right]\hat{x}_a(k); \\ y(k) &= c^\top x(k) = [1\ 0]x(k) \end{aligned}$$

with controller and observer gains K and L chosen to stabilize $(\Phi - \Gamma K^\top)$ and $(\Phi_a^\top - Lc_a^\top)$, respectively.

Proof: By design, the controller/observer forces

$$\hat{x}(k) \rightarrow x(k) \rightarrow 0 \quad \text{and} \quad \hat{x}_d(k) \rightarrow V_d$$

Consequently, $u(k) \rightarrow -V_d$ at a rate controlled by the controller and observer eigenvalues. Furthermore, the chosen least squares set of mitigating actions (11) adjusts the map

$$M_1 = w(w^\top w)^{-1}$$

so that $M_2^\top M_1 = 1$ (see Figure 1), and setting $v^o(k) = -(u(k) + \gamma)$ with

$$u(k) \rightarrow -\hat{x}_d(k) \rightarrow -V_d$$

results in

$$v(k) = V_d - M_2^\top M_1 v^o(k) = V_d - \hat{x}_d + \gamma \rightarrow \gamma$$

The input linearization point is set to $v_s = \gamma$ in simulations.

The design is done assuming standard controllability conditions of the pair $\{\Phi, \Gamma\}$ and the dual system pair $\{\Phi_a^\top, c_a\}$ for the existence of gains K and L. Controllability of $\{\Phi, \Gamma\}$ is guaranteed by $z_{1s}z_{2s} \neq 0$, while with measurement $y(k) = c_a^\top x(k) = [1\ 0\ 0]x(k) = x_1(k)$, that is the small signal susceptible population fraction, controllability of $\{\Phi_a^\top, c_a\}$ is guaranteed by $z_{1s}v_s \neq 0$ and $z_{1s}z_{2s} \neq 0$. Under these conditions, K can be chosen to place the controller eigenvalues, and L may be chosen to arbitrarily place the observer eigenvalues. However, it is interesting to observe that controllability of the dual system is lost when the measured output is $y(k) = x_2(k)$ the small signal infectious population fraction, that is, with $c_a^\top = [0\ 1\ 0]$. Moreover, a reduced-order observer also fails the test.

Now, since $v_s = \gamma > 0$ and $z_{1s} > 0$ but $z_{2s} \rightarrow 0$ as $k \rightarrow \infty$, then controllability is lost only in steady-state. In the SIR context however, the need to design mitigating actions subsides in finite time while $R_e > 1$, that is, $V_d > \gamma$, and hence $z_{2s} \neq 0$. This is due to the fact that in practice we've seen that quarantine window lengths should be minimized to avoid economic, health and other impacts that can be very detrimental to society. Figure 3 combines the idealized SIR model of Figure 1 with the extended state-observer and feedback controller.

III. Simulations and Discussion

Simulations are presented using the Matlab/Simulink package using the parameters listed in Table I. Four mitigating actions are considered each having an assumed

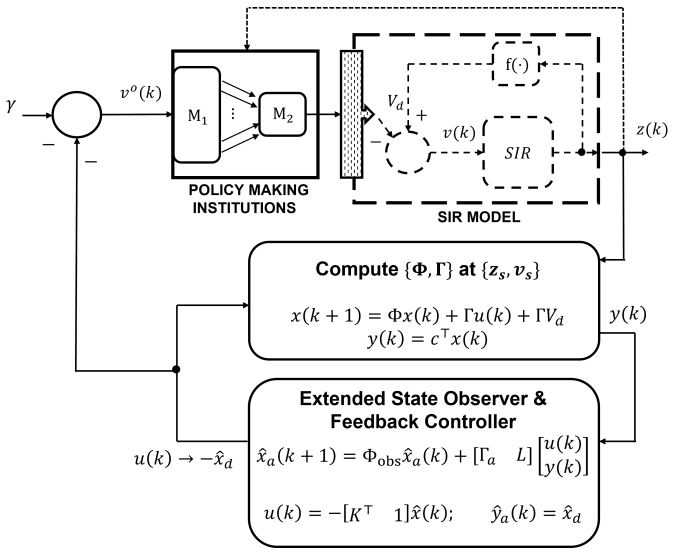

Fig. 3. SIR Extended State Estimator and Feedback Controller.

TABLE I
DISCRETE-TIME HEURISTIC MODEL PARAMETERS

R_e	Basic Reproduction Number	$(0.8, 3.0)$
γ	Recovery Rate (1/days)	$1/14$
U_k	Nominal transmission rate	$(0.0571, 0.2143)$
S_0	Initial Susceptible State	0.88
I_0	Initial Infectious State	0.12
R_0	Initial Removed State	0
a_1	Social-Distancing	$w_1 = 26\%$ reduction in R_e
a_2	Mask-wearing	$w_2 = 50\%$ reduction in R_e
a_3	Lock-Down	$w_3 = 72\%$ reduction in R_e
a_4	Vaccination	$w_4 = 95\%$ reduction in R_e

effectiveness in reducing the reproduction number R_e along the lines of the reports [23], [24].

First, $R_e = 3.0$ ($V_d = 3\gamma = 0.2143$) followed by a step change to $R_e = 1.0$ ($V_d = \gamma = 1/14$) is simulated and discussed next to illustrate the controller/observer performance.

1) Initially, the whole population is considered susceptible. When patient zero seeds the disease, the spread begins, creating a jump in the infectious population fraction I_0, and a step jump in the transmission rate V_d. As illustrated in Figure 2, under no control, $I(k)$ increases, $S(k)$ decreases, and the spread continues adding more cases to $I(k)$ until it reaches a peak, and then naturally overtime the disease disappears with $I(k) \to 0$.
2) The state-feedback controller is designed to place the eigenvalues of $\{\Phi - \Gamma K^\top\}$ at $\lambda = (0.1;\ 0.2)$. Similarly, using $y(k) = x_1(k)$, the extended-state observer design places the eigenvalues of $\{\Phi_a - Lc_a^\top\}$ at $\lambda = (0.05;\ 0.06;\ 0.07)$. The resulting gains are $K^\top = [-95.54; -80.63]$ and $L^\top = [2.69; -148.55; -110.1]$.
3) In an interval of 2-days, the transmission rate is constant $V_d = 3\gamma = 0.2143$ and exhibits a step change at $k = 1$ to $V_d = \gamma = 1/14$.
4) Figure 4 shows the transmission rate V_d and $\hat{V}_d$ from the observer.

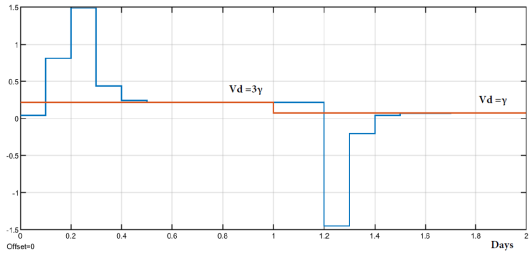

Fig. 4. Transmission Rate V_d and Estimate $\hat{V}_d$.

5) Figures 5 and 6 show the observer error in x_1 and x_2, respectively.

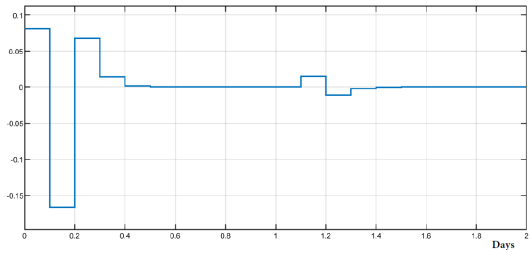

Fig. 5. Observer Error $x_1(k) - \hat{x}_1(k)$.

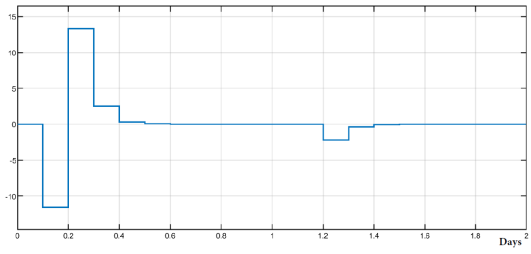

Fig. 6. Observer Error $x_2(k) - \hat{x}_2(k)$.

6) Figure 7 shows the resulting mitigating actions for two values of R_e. As expected, as $R_e \to 1.0$, the action set $a(k) \to 0$. The nature of the SIR control problem requires that in any implementation, the controller/observer system run offline in a faster timescale, hence, only the steady state values of control signals and mitigating actions are relevant to the solution; that is, the transients shown in the simulations are ignored.

The next simulation example closes the loop simulating V_d as a staircase profile resulting in R_e as in Figure 8. It is also assumed that the computed action set is implemented with perfect efficacy weighted as listed in Table I.

1) During each window of time where V_d is a constant, the controller/observer produces the ideal action set profile shown in Figure 9 and resulting $u(k)$ to perfectly match $-V_d$ as in Figure 10.

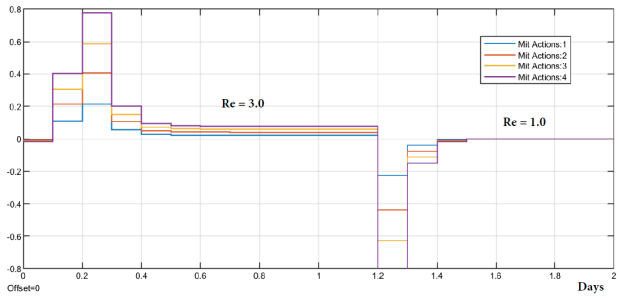

Fig. 7. Mitigating Actions Profile.

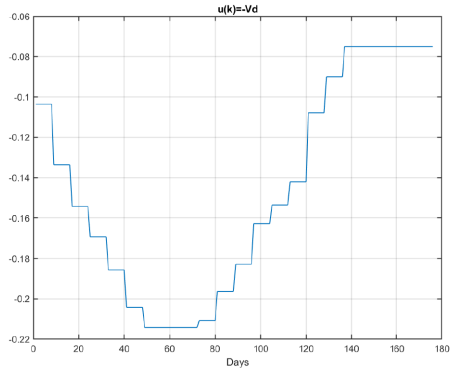

Fig. 10. Small Signal Control - Staircase Transmission Profile.

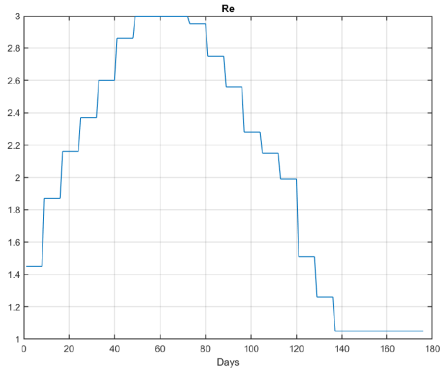

Fig. 8. Basic Reproduction Number - Staircase Transmission Profile.

2) The SIR model response is plotted in Figure 11. A figure of merit used in other works is to reduce the steady state value $z_3(\infty)$ of the removed population fraction [25]. Comparing with the no-control case in Figure 2, there is an almost 50% reduction in the number of removed cases. The infectious population fraction does not exhibit a peak or multiple waves, and simply decreases to zero.
3) These simulations are an idealization because the underlying assumption is the mitigating actions have an immediate and perfect effect on the transmission rate. One way to interpret the mitigating action set and its effect on the transmission rate is to examine what happens when the map M_2 is not ideal. For example, $M_2 = M_2 + \Delta$ where Δ is an implementation disturbance. Figure 12 shows the SIR model response when $\Delta = [0; 0; 0; -0.5M_2(4)]^\top$, that is, a 50% reduction in the efficacy of vaccination a_4. Comparing with the ideal case, the higher $z_3(\infty)$ is an indication of worsened performance, caused by a higher transmission rate or equivalently higher R_e.
In this case, $v(k) = V_d - (M_2 + \Delta)^\top M_1 v^o(k)$ leads to $v(k) \to \gamma + \Delta^\top M_1(\gamma - \hat{x}_d)$. Other scenarios are being constructed considering implementation delays, higher-order SIR models [10], and other types of uncertainties.

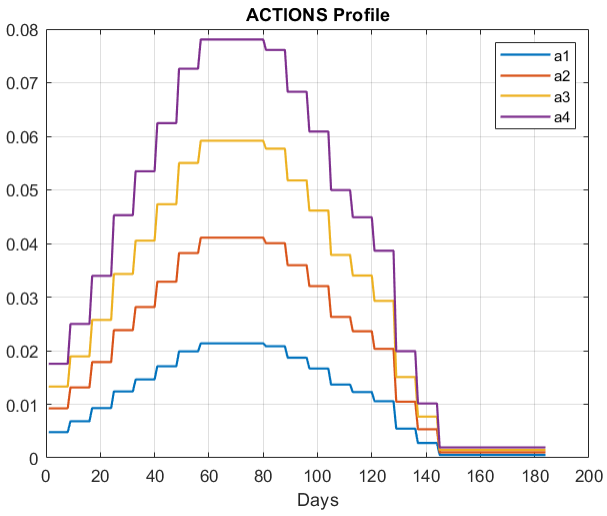

Fig. 9. Ideal Action Set Profile.

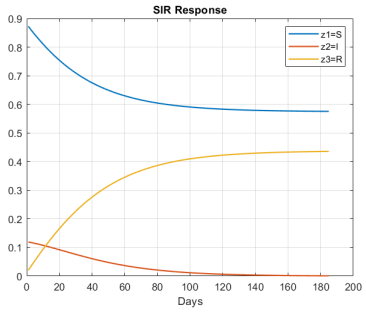

Fig. 11. Ideal SIR Response - Staircase Transmission Profile.

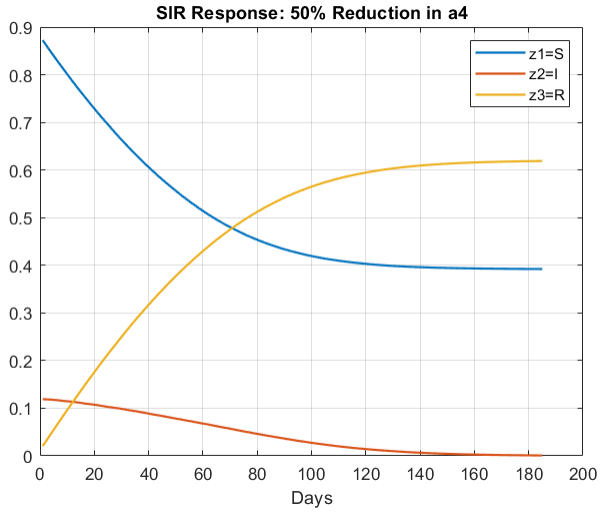

Fig. 12. Non-Ideal SIR Response with 50% Suppressed Vaccination.

IV. Conclusions and Further Work

An SIR model of contagious disease spread was used to illustrate the design of a feedback control policy that adjusts the transmission rate in an effort to maintain the basic reproduction number close to one. A mitigating action set profile can be better managed and the disease spread is mitigated. An extended state observer and state-feedback controller achieve the desired goal. Simulations illustrate the resulting set of four mitigating actions chosen to be social distancing, mask wearing, lock-down and vaccination, when the transmission rate is assumed to be a constant. Insightful comments by a reviewer point to further research: 1) three of the interventions tend to reduce the transmission rate, while vaccinations work to transition individuals from S to R, and a third type of interventions namely pharmaceuticals work to increase gamma but were not used in this paper and should be considered separately; and 2) explore imperfect knowledge of system parameters.

References

[1] J. Cavataio and S. Schnell. *Interpreting SARS-CoV-2 seroprevalence, deaths, and fatality rate — Making a case for standardized reporting to improve communication*. Elsevier Mathematical Biosciences, 333, 2021, {https://doi.org/10.1016/j.mbs.2021.108545}.

[2] H. H. Weiss. *The SIR model and the Foundations of Public Health*. Materials Matemàtics, 2013, pp.1-17, {https://ddd.uab.cat/record/108432}.

[3] H. W. Hethcote. *The Mathematics of Infectious Diseases*. SIAM Review, V. 42, No. 4, (Dec. 2000), pp.599-653.

[4] F. Brauer. *Mathematical epidemiology: Past, present, and future*. KeAi Infectious Disease Modelling, V.2, 2017, pp.113-127.

[5] Qianying Lin et al. *A conceptual model for the coronavirus disease 2019 (COVID-19) outbreak in Wuhan, China with individual reaction and governmental action*. International Journal of Infectious Diseases, Elsevier, V.93, 2020, pp.211-216.

[6] W.E. Fitzgibbon, J.J. Morgan, G.F. Webb, and Y. Wu. *Predicting the end-stage of the COVID-19 epidemic in Brazil*. June 2020. medRxiv doi: {https://doi.org/10.1101/2020.05.28.20116103}

[7] Y.C. Chen, P.E. Lu, C.S. Chang, and T.H. Liu. *A time-dependent SIR model for COVID-19 with undetectable infected persons*. Cornell University, Populations and Evolution, April 2020, {arXiv:2003.00122}.

[8] A. Arenas, W. Cota, J. Gómez-Gardeñes et al. *A mathematical model for the spatiotemporal spreading of COVID-19*. March 2020, medRxiv, doi: {https://doi.org/10.1101/2020.03.21.20040022}

[9] P. Savi, M.A. Savi, and B. Borges, *A mathematical description of the dynamics of the coronavirus disease 2019 (COVID-19): a case study of Brazil*. Cornell University, Populations and Evolution, April 2020, URL: {https://arxiv.org/abs/2004.03495}

[10] M. A. Bahloul, A. Chahid, and T-M Laleg-Kirati. *Fractional Order SEIQRDP Model for Simulating the Dynamics of COVID-19 Epidemic*. IEEE Open Journal of Engineering in Medicine and Biology. V.1, 2020, pp.249-256.

[11] Z. Liu, P. Magal, and G. Webb. *Predicting the number of reported and unreported cases for the COVID-19 epidemics in China, South Korea, Italy, France, Germany, and United Kingdom*. Journal of Theoretical Biology, V.509, January 2021. {https://doi.org/10.1016/j.jtbi.2020.110501}

[12] V. Z. Marmarelis. *Predictive Modeling of Covid-19 Data in the US: Adaptive Phase-Space Approach*. IEEE Open Journal of Engineering in Medicine and Biology. V.1, 2020, pp.207-213.

[13] U. Ledzewicz and H. Schättler. *On optimal singular controls for a general SIR-model with vaccination and treatment*. American Institute of Mathematical Sciences, Discrete and Continuous Dynamical Systems, V.2011, Special, pp.981-990. {http://dx.doi.org/10.3934/proc.2011.2011.981}

[14] M. Elhia, M. Rachik, and E. Benlahmar. *Optimal Control of an SIR Model with Delay in State and Control Variables*. Hindawi Publishing Corporation, ISRN Biomathematics, Volume 2013, Article ID 403549, 7 pages {http://dx.doi.org/10.1155/2013/403549}

[15] L. Bolzoni, E. Bonacini, C. Soresina, and M. Groppi. *Time-optimal control strategies in SIR epidemic models*. Elsevier Mathematical Biosciences, 292, 2017, pp.86-96 {http://dx.doi.org/10.1016/j.mbs.2017.07.011}.

[16] P.Di Giamberardino, D. Iacoviello, F. Papa, and C. Sinisgalli. *Dynamical evolution of COVID-19 in Italy with an evaluation of the size of the asymptomatic infective population*. IEEE Journal of Biomedical and Health Informatics (Early Access), July 2020, {DOI: 10.1109/JBHI.2020.3009038}

[17] G. Stewart, K. Van Heusden, and G. A. Dumont. *How Control Theory Can Help Us Control COVID-19*. IEEE Spectrum, July 17, 2020, {spectrum.ieee.org/how-control-theory-can-help-control-covid19}

[18] C. Castilho, J. A. M. Gondim, M. Marchesin, and M. Sabeti. *Assessing the efficiency of different control strategies for the coronavirus (COVID-19) epidemic*. April 2020. {arXiv:2004.03539v1 [q-bio.PE]}

[19] N. M. Gatto and H. Schellhorn. *Optimal control of the SIR model in the presence of transmission and treatment uncertainty*. Elsevier Mathematical Biosciences, 333, 2021, {https://doi.org/10.1016/j.mbs.2021.108539}.

[20] E. Barbieri, W.E. Fitzgibbon, and J. Morgan. *New Insights into an Epidemic SIR Model for Control and Public Health Intervention*. IEEE Conference on Control Technology and Applications (CCTA), San Diego, CA, Aug 8-11, 2021, pp.150-155.

[21] E. Barbieri and V. Tzouanas. *On Feedback Control for a Family of Infectious Disease SIR Models*. IEEE Conference on Decision and Control (CDC), Austin, TX, Dec 13-17, 2021.

[22] B. Friedland. *Control System Design - An Introduction to State-Space Methods*. McGraw-Hill Book Company, New York, 1986.

[23] L. Peeples *Face masks: what the data say*. Nature, V.586, pp.186-189, 2020.

[24] S. Flaxman, S. Mishra, A. Gandy et. al. *Estimating the effects of non-pharmaceutical, interventions on COVID-19 in Europe*. Nature, V.584, pp.257-261, June 2020.

[25] Y. Feng, G. Iyer, and L. Lei. *Scheduling fixed length quarantines to minimize the total number of fatalities during an epidemic*. Journal of Mathematical Biology, 2021, V.82, No.69, pp.1-17.